

Fuel Economy and String Stability: A Dynamics Based Study on Heavy Road Vehicle Platoons

K. B. Devika

Department of Engineering Design
IIT Madras
Chennai, India
devikakb@gmail.com

Shankar C. Subramanian

Department of Engineering Design
IIT Madras
Chennai, India
shankaram@iitm.ac.in

Abstract—The intervehicular distances between the constituent vehicles are highly significant in deciding the fuel economy of vehicular platoon formations. This paper studies the effect of time-headway, which characterizes the intervehicular distance, on the fuel economy of Heavy Commercial Road Vehicle (HCRV) platoons. The study has been conducted using a complete vehicle dynamics model, making it a realistic approach that could be adopted for planning HCRV platoon formations. A relationship between time-headway and fuel cost has been obtained for HCRV platoons operating at various longitudinal speeds. In addition, the aspect of string stability of the platoon to various speed perturbation signals has also been investigated for various time-headway magnitudes, considering different road conditions. It has been observed that there lies a minimum magnitude of time-headway to guarantee string stability, depending upon the speed perturbation and road conditions. This study can hence be viewed as a systematic approach for the selection of time-headway for fuel economic and string stable platoon formations under various operating conditions.

Index Terms—fuel savings, heavy commercial road vehicle, platoon, string stability

I. INTRODUCTION

Increased freight transportation all over the world increases the demand for more sustainable solutions. Heavy Commercial Road Vehicle (HCRV) platooning is a potential solution for the same [1], [2]. A platoon is a convoy of vehicles that travel at close intervehicular distances so as to reduce the aerodynamic drag and hence the fuel consumption [3]. In addition to this aspect, its ability to operate with minimum utilisation of road infrastructure, makes vehicle platooning a promising freight transportation strategy [4].

The notion of string stability is important as far as the autonomous operation of platoons is concerned [5], [6]. For string stable platoon operation, any speed perturbation that acts on the platoon should get attenuated along the platoon. To ensure this, a controller that is capable of attenuating the spacing error between a pair of vehicles in the event of any bounded speed perturbation is required [7]. String stable controllers are usually designed such that the inter-vehicular spacing is maintained at a constant value, leading to a constant spacing policy [8], [9] or by allowing it to vary, but in a bounded manner, known as constant time-headway (CTH) policy [10], [11]. In CTH policy, the intervehicular distance between the consecutive vehicles in the platoon depends

upon the magnitude of time-headway. Hence, the reduction in aerodynamic drag and the reduction in fuel consumption also depend on the time-headway. In this context, this paper studies the effect of variation in time-headway on fuel economy of the platoon. To carry out this study, a complete vehicle dynamics model including aerodynamic drag and rolling resistance, tyre model, wheel dynamics, and brake/powertrain actuator dynamics has been used. The use of such a complete vehicle model would help to emulate the real vehicle platoon operation and hence the conclusions drawn from the study would be more realistic.

The variation in time-headway changes the intervehicular distance in the platoon and hence would significantly affect the string stability [12]–[14]. In this regard, in addition to the impact of time-headway on fuel economy, its impact on string stability has also been investigated in this paper. Sliding Mode Control (SMC), which is a robust control strategy, is an established candidate for the design of string stable controllers for vehicular platoons [8], [10], [15]. A string stable controller using Power Rate Exponential Reaching Law (PRERL) based SMC has been developed by the authors to establish string stable HCRV platoon operation under different road and vehicle conditions [16]. This design approach was based on a complete vehicle dynamics model and has been found to be an adequate controller for emulating real vehicle platoon operation. Hence, this controller has been used in this study to investigate string stability for various time-headway operations. String stable operation of HCRV platoons has been investigated for different road conditions and for different lead vehicle deceleration profiles, by changing the time-headway from a minimum value to higher values. Finally, the minimum time-headway required to establish string stability in each operating conditions has been obtained.

This paper is organised as follows: The platoon model incorporating the complete vehicle dynamics is explained in section II. A discussion on the dependency between intervehicular distances and fuel consumption in vehicular platoons is presented in section III. A review on string stable control design using SMC is given in section III. The study on the dependency of time-headway on fuel cost and string stability along with relevant results are presented in section IV. Section V concludes the paper.

II. PLATOON MODEL

The HCRV platoon under consideration consists of $N + 1$ vehicles, with one leader vehicle and N followers. Following are the major assumptions made in this study:

- The vehicles travel on a straight and flat road.
- Only longitudinal dynamics of the vehicle is considered.
- The tyre model parameters and vehicle parameters are assumed to be known.
- There is equal distribution of load on the left and right wheels of a specific axle of the vehicle.

A. Vehicle Model

The dynamics of the i^{th} follower vehicle in the platoon can be represented as

$$\begin{aligned}\dot{x}_i(t) &= v_i(t), \\ \dot{v}_i(t) &= \Lambda(v_i(t), \tau_i(t)),\end{aligned}\quad (1)$$

where, $i = 1 \dots N$, $x_i(t)$ and $v_i(t)$ represent the position and speed of the vehicle, and $\tau_i(t)$ represent the drive/brake torque of the vehicle. Here, $\Lambda(v_i(t), \tau_i(t))$ is a nonlinear function in $v_i(t)$, and $\tau_i(t)$ and is given by

$$\Lambda(v_i(t), \tau_i(t)) = \frac{1}{m_i} (F_{xfi}(\lambda_{fi}(t)) + F_{xri}(\lambda_{ri}(t)) - F_{Ri}(t)). \quad (2)$$

Here, $F_{xfi}(\lambda_{fi}(t))$ and $F_{xri}(\lambda_{ri}(t))$ represent the longitudinal forces at the front and rear tyre-road interface respectively, and $\lambda_{fi}(t)$ and $\lambda_{ri}(t)$ represent the longitudinal slip ratios of front and rear wheels respectively, which are given by

$$\begin{aligned}\lambda_{fi}(t) &= \frac{v_i(t) - r_i \omega_{fi}(t)}{v_i(t)}, \\ \lambda_{ri}(t) &= \frac{v_i(t) - r_i \omega_{ri}(t)}{v_i(t)},\end{aligned}\quad (3)$$

where, r_i is the tyre radius. From the wheel dynamics, ω_{fi} and ω_{ri} can be obtained as,

$$\begin{aligned}\dot{\omega}_{fi}(t) &= \frac{1}{I_{fi}} (\tau_{fi}(t) - r_i F_{xfi}(t)), \\ \dot{\omega}_{ri}(t) &= \frac{1}{I_{ri}} (\tau_{ri}(t) - r_i F_{xri}(t)),\end{aligned}\quad (4)$$

where, I_{fi} and I_{ri} are the moment of inertia of front and rear wheels respectively, $\tau_{fi}(t)$ and $\tau_{ri}(t)$ are the transmitted torques to the front and rear wheels respectively. Now, the resistive force, $F_{Ri}(t)$ in (2) can be expressed as,

$$F_{Ri}(t) = F_{ai}(t) + R_{xfi}(t) + R_{xri}(t), \quad (5)$$

where, $F_{ai}(t)$ represents the force due to aerodynamic drag, and R_{xfi} and R_{xri} are the forces due to rolling resistance at the front and rear wheels respectively. The aerodynamic drag force is characterized by the air density, ρ , the aerodynamic drag coefficient, $C_{Di}(t)$, and the vehicle frontal area, a_{fi} . The rolling resistance is characterized by the rolling resistance coefficient, and the normal forces on both front and rear tyres,

represented respectively by $F_{zfi}(t)$ and $F_{zri}(t)$. The normal forces at the tyre-road interface are given by

$$\begin{aligned}F_{zfi}(t) &= \frac{m_i g l_r - F_{ai}(t) h_a - m_i a_i(t) h_{cg}}{l_f + l_r}, \\ F_{zri}(t) &= \frac{m_i g l_f + F_{ai}(t) h_a + m_i a_i(t) h_{cg}}{l_f + l_r},\end{aligned}\quad (6)$$

where, $a_i(t)$ is the longitudinal acceleration, h_{cg} is the height of the C.G. of the vehicle, h_a is the height of the location at which the equivalent aerodynamic force acts, and l_f and l_r are the longitudinal distance of the front axle and rear axle from the C.G. of the vehicle.

1) *Actuator Dynamics*: The transfer function of the actuator dynamics [11] is given by

$$P(s) = \frac{\tau_i(s)}{\tau_{des}(s)} = \frac{1}{1 + \tau_d s} e^{-T_d s}, \quad (7)$$

where, τ_d is the time constant, and T_d is the time delay, and τ_{des} and τ_i represent the demanded torque and actual torque developed, respectively. In this paper, $\tau_d = 260$ ms and $T_d = 45$ ms have been used to represent brake/powertrain time constant and time delay [16]. In order to compensate actuator time delay, Padé approximation has been used in this paper [17]. Using the first order Padé approximation, the actuation model (7) can be rewritten as

$$P(s) \approx \frac{(2 - T_d s)}{(1 + s \tau_d)(2 + T_d s)}. \quad (8)$$

Considering the torque dynamics in the front wheels of the i^{th} vehicle, the state space equation of (8) can be written as

$$\begin{bmatrix} \dot{\tau}_{1fi}(t) \\ \dot{\tau}_{2fi}(t) \end{bmatrix} = \begin{bmatrix} 0 & 1 \\ \frac{-2}{\tau_d T_d} & -(\frac{1}{\tau_d} + \frac{2}{T_d}) \end{bmatrix} \begin{bmatrix} \tau_{1fi}(t) \\ \tau_{2fi}(t) \end{bmatrix} + \begin{bmatrix} 0 \\ 1 \end{bmatrix} \tau_{desfi}(t), \quad (9)$$

$$\tau_{fi}(t) = \begin{bmatrix} \frac{2}{T_d \tau_d} \\ \frac{-1}{\tau_d} \end{bmatrix} \cdot \begin{bmatrix} \tau_{1fi}(t) \\ \tau_{2fi}(t) \end{bmatrix}, \quad (10)$$

and the torque dynamics in the rear wheels of the i^{th} vehicle can be written as

$$\begin{bmatrix} \dot{\tau}_{1ri}(t) \\ \dot{\tau}_{2ri}(t) \end{bmatrix} = \begin{bmatrix} 0 & 1 \\ \frac{-2}{\tau_d T_d} & -(\frac{1}{\tau_d} + \frac{2}{T_d}) \end{bmatrix} \begin{bmatrix} \tau_{1ri}(t) \\ \tau_{2ri}(t) \end{bmatrix} + \begin{bmatrix} 0 \\ 1 \end{bmatrix} \tau_{desri}(t), \quad (11)$$

$$\tau_{ri}(t) = \begin{bmatrix} \frac{2}{T_d \tau_d} \\ \frac{-1}{\tau_d} \end{bmatrix} \cdot \begin{bmatrix} \tau_{1ri}(t) \\ \tau_{2ri}(t) \end{bmatrix}. \quad (12)$$

Now, on substituting $\tau_{1fi}(t)$, $\tau_{2fi}(t)$ from (10) and (12) in (4), the wheel dynamics can be expressed as

$$\begin{aligned}\dot{\omega}_{fi}(t) &= \frac{1}{I_{fi}} \left(\frac{2}{T_d \tau_d} \tau_{1fi}(t) - \frac{1}{\tau_d} \tau_{2fi}(t) - r_i F_{xfi}(t) \right), \\ \dot{\omega}_{ri}(t) &= \frac{1}{I_{ri}} \left(\frac{2}{T_d \tau_d} \tau_{1ri}(t) - \frac{1}{\tau_d} \tau_{2ri}(t) - r_i F_{xri}(t) \right).\end{aligned}\quad (13)$$

Considering the above discussed complete vehicle model including actuator dynamics, the entire state space representation for a single vehicle in the platoon can be represented in the following state vector form:

$$\dot{\Phi}_i(t) = f(\Phi_i(t), \mathbf{u}_i(t)), \quad (14)$$

where, $\Phi_i(t)$ and $\mathbf{u}_i(t)$ represent the state vector and the input vector respectively, given by

$$\Phi_i(t) = [x_i(t) \ v_i(t) \ \omega_{fi}(t) \ \omega_{ri}(t) \ \tau_{1fi}(t) \ \tau_{2fi}(t) \ \tau_{1ri}(t) \ \tau_{2ri}(t)]^T, \quad \mathbf{u}_i(t) = [\tau_{desfi}(t) \ \tau_{desri}(t)]^T.$$

B. Tyre Model

The Magic Formula (MF) tyre model [18] that gives a good representation of forces acting on the tyre-road interface for a wide range of operating conditions has been used in this paper. Using the MF model, for a single tyre, the longitudinal force can be represented as,

$$F_x(\lambda(t)) = D \sin(C \tan^{-1}(B\lambda_x - E(B\lambda_x(t) - \tan^{-1} B\lambda_x(t)))) + S_V, \quad (15)$$

where, $\lambda_x(t) = \lambda(t) + S_H$.

In this work, the MF model parameters, B, C, D, E, S_H , and S_V were obtained from the vehicle dynamic simulation software, IPG TruckMaker®.

III. DEPENDENCY BETWEEN INTERVEHICULAR DISTANCE AND FUEL CONSUMPTION

The aerodynamic drag force for each vehicle in the platoon is given by,

$$F_{ai}(t) = \rho \ a_{fi} \ C_{Di}(t) \frac{v_i(t)^2}{2}, \quad (16)$$

where, ρ is the density of air, $C_{Di}(t)$ is the aerodynamic drag coefficient and a_{fi} is the frontal area of the vehicle. The frontal area is assumed to be same for each vehicle ($a_{fi} = a_f$), considering a homogeneous HCRV platoon. The drag coefficient of each vehicle in the platoon depends on the intervehicular distance $d_i(t)$. In [19], a nonlinear relationship between $C_{Di}(t)$ and $d_i(t)$ has been developed through empirical methods and it has been used in this paper. This relationship is given by

$$C_{Di}(t) = C_{D0}(\gamma_1 d_i(t)^{\gamma_2} + \gamma_3). \quad (17)$$

The drag coefficient of any individual vehicle (not operating in a platoon formation) is given as C_{D0} , and the parameters γ_1, γ_2 , and γ_3 are obtained empirically [19].

The fuel cost associated with the longitudinal motion of an HCRV, during drive mode is assumed to be proportional to the consumed energy, which can be described as [3]:

$$f_{ci} = K_{ei} \int (F_{xfi}(t) + F_{xri}(t)) v_i(t) dt, \quad (18)$$

where, K_{ei} is the energy conversion constant based on energy density of diesel and engine combustion efficiency of the individual HCRVs in the platoon, and the value of K_{ei} is chosen to be 1 [3].

IV. CONSTANT TIME-HEADWAY BASED STRING STABLE CONTROLLER DESIGN

As discussed earlier, the platoon consists of $N+1$ vehicles, with one leader and N followers. The longitudinal motion of the leader vehicle is characterized by

$$\dot{x}_0(t) = v_0(t), \quad (19)$$

where, $x_0(t)$ and $v_0(t)$ are the position and longitudinal speed of the leader vehicle. From equations (1) and (2), the longitudinal motion of the follower vehicles is described by

$$\begin{aligned} \dot{x}_i(t) &= v_i(t), \\ \dot{v}_i(t) &= \frac{1}{m_i} (F_{xfi}(\lambda_{fi}(t)) + F_{xri}(\lambda_{ri}(t)) - F_{Ri}(t)), \end{aligned} \quad (20)$$

where, $i = 1 \dots N$. On substituting $F_{xfi}(\lambda_{fi}(t))$ and $F_{xri}(\lambda_{ri}(t))$ from equation (4) in equation (20), one can obtain the follower vehicle dynamics as,

$$\begin{aligned} \dot{v}_i(t) &= \frac{1}{m_i} \left[\frac{1}{r_i} (\tau_{fi}(t) - I_{fi} \dot{\omega}_{fi}(t)) + \frac{1}{r_i} (\tau_{ri}(t) - \right. \\ &\quad \left. I_{ri} \dot{\omega}_{ri}(t)) - F_{Ri}(t) \right]. \end{aligned} \quad (21)$$

For the considered platoon of HCRVs, the spacing between a pair of vehicles is given by

$$d_i(t) = x_{i-1}(t) - x_i(t), \quad (22)$$

and the desired inter-vehicular distance is defined as

$$s_d(t) = s_o + h_i v_i(t), \quad (23)$$

where, s_o and h_i represent standstill spacing and the time-headway respectively. In this approach, the time-headway is taken as constant and it depends upon the desired spacing between the vehicles. Now, the spacing error between two consecutive vehicles can be written as

$$e_i(t) = d_i(t) - s_d(t). \quad (24)$$

The control objective here is to drive the spacing error between consecutive vehicles to zero, such that,

$$d_i(t) = s_o + h_i v_i(t). \quad (25)$$

A. Sliding Mode Controller Design

The following sliding function has been defined for driving the spacing error zero and is given by [10]:

$$s_i(t) = e_i(t) + \int_0^t \kappa e_i(\tau) d\tau. \quad (26)$$

The term, κ is a positive constant and it defines the slope of the sliding function. The selection of the above sliding function with an integral term would avoid the use of derivative of acceleration (jerk) data from preceding vehicles. The sliding function (26) has been defined such that the inter-vehicular spacing error between two consecutive vehicles to zero. However, to achieve string stability, the sliding function should be

redefined for attenuating the spacing error propagation [10]. The redefined sliding function is given by

$$S_i(t) = \begin{cases} qs_i(t) - s_{i+1}(t), & i = 1, \dots, N-1 \\ qs_i(t), & i = N \end{cases}, \quad (27)$$

where, $q > 0$.

For designing a robust and smooth (chattering-free) SMC control action, PRERL structure [20] has been used in this paper, which is given by

$$\dot{S}_i(t) = -\frac{\psi}{\delta_0 + (1 - \delta_0)e^{-\alpha|S_i(t)|^p}} |S_i(t)|^\chi \text{sign}(S_i(t)). \quad (28)$$

Here, $\psi > 0$ is the controller gain, $\delta_0 < 1$, $\alpha > 0$, $0 < \chi < 0.5$ and $p > 0$ are controller parameters that affect the reaching time and chattering mitigation properties.

Now, during braking maneuvers, the proportion of the brake torque applied on the front and rear wheels follow a linear proportion, β , such that

$$\frac{\tau_{fi}(t)}{\tau_{ri}(t)} = \frac{\beta}{1 - \beta}. \quad (29)$$

The above linear relationship is now used in equation (21) to obtain

$$\begin{aligned} \dot{v}_i(t) &= \tau_{ri}(t) \left[\frac{1}{m_i r_i} \left(1 + \frac{\beta}{1 - \beta} \right) \right] - \\ &\frac{1}{m_i r_i} (I_{fi} \dot{\omega}_{fi}(t) + I_{ri} \dot{\omega}_{ri}(t)) - \frac{F_{Ri}(t)}{m_i}. \end{aligned} \quad (30)$$

On obtaining the first derivatives of equations (27) and (26), and using the vehicle dynamics equation (30) and the PRERL structure equation (28), the control input, $\tau_{ri}(t)$ can be obtained as

$$\begin{aligned} \tau_{ri}(t) &= \frac{-1}{qh_i \left[\frac{1}{m_i r_i} \left(1 + \frac{\beta}{1 - \beta} \right) \right]} \\ &\left[\frac{-\psi}{\delta_0 + (1 - \delta_0)e^{-\alpha|S_i(t)|^p}} |S_i(t)|^\chi \text{sign}(S_i(t)) \right. \\ &- q(v_{i-1}(t) - v_i(t)) - q\kappa e_i(t) + \dot{e}_{i+1}(t) + \kappa e_{i+1}(t) \\ &\left. + qh_i \left[\frac{-1}{m_i r_i} (I_{fi} \dot{\omega}_{fi}(t) + I_{ri} \dot{\omega}_{ri}(t)) - \frac{F_{Ri}(t)}{m_i} \right] \right] \\ &i = 1, \dots, N-1, \end{aligned} \quad (31)$$

$$\begin{aligned} \tau_{rN}(t) &= \frac{-1}{qh_N \left[\frac{1}{m_N r_N} \left(1 + \frac{\beta}{1 - \beta} \right) \right]} \\ &\left[\frac{-\psi}{\delta_0 + (1 - \delta_0)e^{-\alpha|S_N(t)|^p}} |S_N(t)|^\chi \text{sign}(S_N(t)) \right. \\ &- q(v_{N-1}(t) - v_N(t)) - q\kappa e_N(t) + qh_N \left[\frac{-1}{m_N r_i} \right. \\ &\left. \left. (I_{fN} \dot{\omega}_{fN}(t) + I_{rN} \dot{\omega}_{rN}(t)) - \frac{F_{RN}(t)}{m_N} \right] \right]. \end{aligned} \quad (32)$$

Now, using (29), the torque inputs for the front wheels can be obtained.

Considering a rear wheel driven HCRV, during drive mode, $\tau_{fi}(t) = 0$, $\tau_{ri}(t) = \tau_i(t)$. By substituting $\tau_{fi}(t) = 0$ in (21), and by following the same controller design steps as presented above, the torque inputs during drive mode can also be obtained. For brevity, these inputs are not explicitly derived in this paper.

V. RESULTS AND DISCUSSIONS

In order to study the fuel savings and string stability aspects of HCRV platoons, a five vehicle platoon, with one leader and four follower HCRVs has been considered. All the HCRVs in the platoon were assumed to be homogeneous and hence, the vehicle parameters shown in Table I have been used for realising all the follower vehicles. The complete vehicle

TABLE I
VEHICLE PARAMETERS.

Parameter	Value
Vehicle mass, m	16200 kg
Wheel radius, r	0.53 m
C.G. height, h_{cg}	1.3 m
Front axle distance from the C.G, l_f	3.4 m
Rear axle distance from the C.G, l_r	2 m
Moment of inertia of front wheels, I_f	10 kgm ²
Moment of inertia of rear wheels, I_r	20 kgm ²

dynamics model and the string stable controller have been programmed in MATLAB SIMULINK®.

Initially, the effect of change in time-headway on fuel consumption of HCRVs in the platoon has been studied. This study has been conducted for a platoon operating on a straight and level road with constant speeds. The following conditions are considered:

- Different vehicle speeds - 70 km/h, 60 km/h and 50 km/h.
- Different road conditions - $\mu = 0.8$ and $\mu = 0.5$.

For each of the considered scenario, time headway, h_i has been varied from 0.5 s to higher values, where platooning is feasible in terms of fuel cost. Fuel cost for operating each vehicle in the platoon for a distance of 500 m (with constant speed) is calculated. For calculating the fuel cost, expression given by (18) has been used. Using the presented platoon framework, plots that characterize the variation in the fuel cost as a function of time headway for different operating speeds have been obtained as shown in Fig. 1.

It can be observed that, after a particular threshold value of h_i , the fuel cost remains constant. This is due to the fact that, the reduction in aerodynamic drag between the vehicles and hence the fuel cost could be achieved only if the intervehicular distance is small. Increase in h_i would result in increased intervehicular distance and hence increased fuel consumption. After a critical value of intervehicular distance (corresponding to a critical value of time-headway, $h_{i_{crit}}$), the advantage of being in a platoon in terms of reduced fuel consumption could not be achieved. It was also found that beyond the value of $h_{i_{crit}}$, the fuel consumption for each vehicle in the platoon would be the same as that of a vehicle operating individually rather than in a platoon formation.

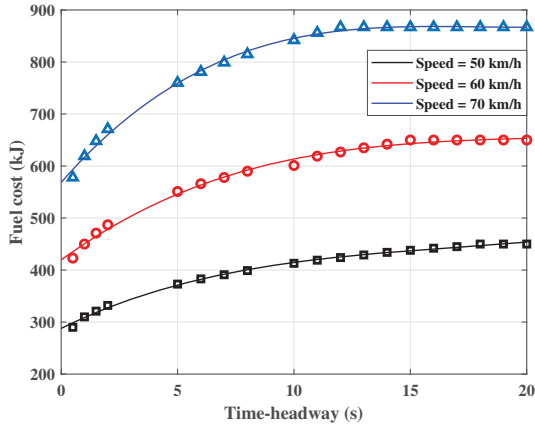


Fig. 1. Variation between time headway and fuel cost

From this study, it was found that, for any given speed and for a set of fixed operating conditions, it is possible to present equation (18) in terms of h_i alone. From the data obtained using equation (18) for different h_i values, and using curve fitting, the variation in fuel cost with respect to the time-headway was found to be following a cubic function, and can be presented as,

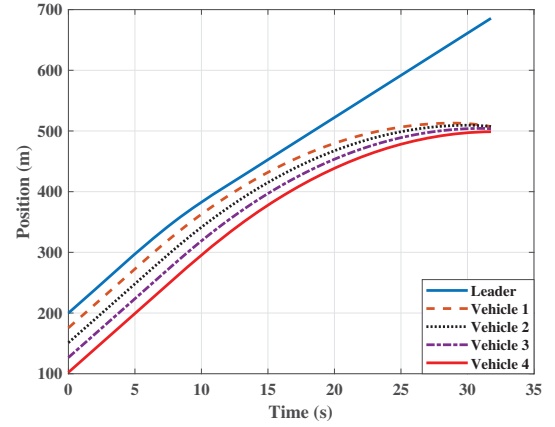
$$f_c(h_i) = f_{c0} + c_1 h_i + c_2 h_i^2 + c_3 h_i^3. \quad (33)$$

Here f_{c0} represents the minimum fuel cost, c_1 , c_2 , and c_3 are coefficients obtained via curve fitting. This simplified expression for fuel cost as a function of time-headway can suitably be used while planning fuel efficient platoon operation.

Another important aspect while realising platoon operation is the notion of string stability. Time headway should be chosen for vehicle platooning in such a way that maximum fuel efficiency is achieved while not compromising on string stability. In this regard, another study has also been conducted in order to investigate the relationship between time-headway and string stability. The issue of string stability becomes critical when the vehicles in the platoon undergo a braking maneuver. In such scenarios, the magnitude of time-headway is significant in establishing string stability. In this regard, various lead vehicle braking maneuvers that act as perturbations to the entire platoon operation have been considered and tested for string stability. The test matrix and observations corresponding to the vehicle speed of 70 km/h are presented in Table II. The fixed set of controller parameter set given by: $\psi = 1$, $\delta_o = 0.1$, $\alpha = 50$, $p = 1$, $\chi = 0.5$, $\kappa = 0.1$ and $q = 0.9$ were used to design PRERL based string stable controller. The vehicle speed of 70 km/h has been considered here to show a worst case platoon operation, in which the constituent HCRVs operate at high speed and hence more prone towards string instability. The lead vehicle was assumed to undergo three different braking maneuvers of different decelerations. The minimum value of time-headway was set as 0.5 s. When the lead vehicle deceleration is as low as 0.5 m/s^2 , for high μ ($\mu = 0.8$) road, string stability was achieved for h_i values as

TABLE II
TEST MATRIX AND OBSERVATIONS

Longitudinal Speed (km/h)	Lead Vehicle Deceleration (m/s^2)	Road	String stability
70 km/h	0.5	0.8	YES - if $h_i \geq 0.5$
	0.5	0.5	YES - if $h_i \geq 2$
	1	0.8	YES - if $h_i \geq 0.5$
	1	0.5	YES - if $h_i \geq 3.5$
	2	0.8	YES - if $h_i \geq 2$
	2	0.5	YES - if $h_i \geq 5$

Fig. 2. Plots showing string instability at $\mu = 0.5$, $h = 1$ s, for lead vehicle deceleration of 1 m/s^2 .

low as 0.5 s. However, it was found that string stability could be achieved only for $h_i \geq 2$ s on a road of $\mu = 0.5$. Similar observations can be seen when the lead vehicle deceleration was increased to 1 m/s^2 and 2 m/s^2 . A sample case, when $\mu = 0.5$, $h_i = 1$ s and lead vehicle deceleration of 1 m/s^2 is shown in Fig. 2, showing string instability due to low value of h_i . The results corresponding to the same case as above, but with $h_i = 3.5$ s are shown in Fig. 3 and Fig. 4. The longitudinal speed and position profiles show the string stable operation while operating with $h_i = 3.5$ s.

It is to be noted that for high deceleration values and for low μ cases, the situation is quite critical, demanding large values of time-headway for stable platoon operation. This vehicle dynamics and operating condition dependent design approach help one to choose the feasible ranges of h_i that could establish string stable platoon operation on pre-defined routes. Along with this insight on h_i selection, one can easily get a quantitative estimate of the fuel consumption from the empirical relationship presented by (33).

VI. CONCLUSION

Fuel economy and string stability are two important aspects that need to be taken into account while planning efficient vehicular platoons. In this regard, this paper investigated the effects of variation in time-headway on fuel cost and string stability. The major contributions of this paper are the following:

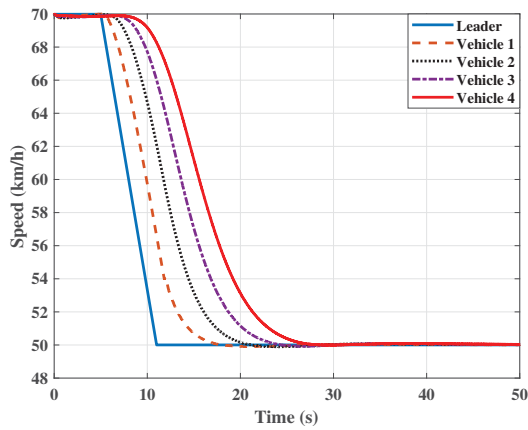


Fig. 3. Speed tracking profiles for $\mu = 0.5$, $h = 3.5$ s, for lead vehicle deceleration of 1 m/s^2 .

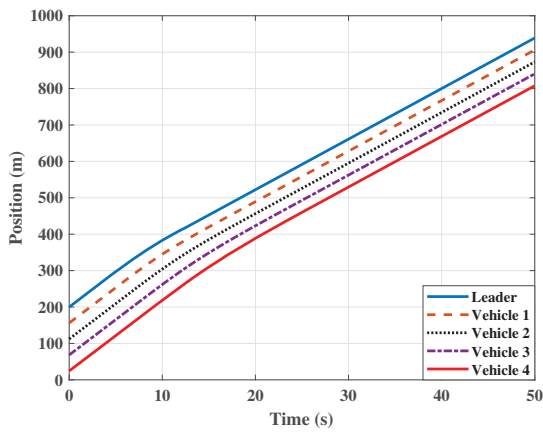


Fig. 4. Position profiles for $\mu = 0.5$, $h = 3.5$ s, for lead vehicle deceleration of 1 m/s^2 .

- A study on the relationship between time-headway and fuel economy in HCRV platoons has been carried out.
- A relationship between time-headway and fuel cost has been obtained.
- A study on the impact of time-headway on string stability has been carried out.
- String stable operation of HCRV platoon has been investigated for different lead vehicle braking maneuvers and the minimum time-headway required to establish string stability in each case has been obtained.

Using the approach presented in this paper, with the available route information, it is possible to choose time-headway values that give minimum fuel operation without compromising on string stability.

ACKNOWLEDGEMENTS

The authors thank the Ministry of Skill Development and Entrepreneurship, Government of India, for funding through the grant EDD/14-15/023/MOLE/NILE.

REFERENCES

- [1] S. Sivanandham and M. Gajanand, "Platooning for sustainable freight transportation: an adoptable practice in the near future?" *Transport Reviews*, pp. 1–26, 2020.
- [2] A. Alam, B. Besselink, V. Turri, J. Mårtensson, and K. H. Johansson, "Heavy-duty vehicle platooning for sustainable freight transportation: A cooperative method to enhance safety and efficiency," *IEEE Control Systems Magazine*, vol. 35, no. 6, pp. 34–56, 2015.
- [3] K.-Y. Liang, J. Mårtensson, and K. H. Johansson, "Heavy-duty vehicle platoon formation for fuel efficiency," *IEEE Transactions on Intelligent Transportation Systems*, vol. 17, no. 4, pp. 1051–1061, 2015.
- [4] J. Lioris, R. Pedarsani, F. Y. Tascikaraoglu, and P. Varaiya, "Platoons of connected vehicles can double throughput in urban roads," *Transportation Research Part C: Emerging Technologies*, vol. 77, pp. 292–305, 2017.
- [5] D. Swaroop, J. K. Hedrick, C. Chien, and P. Ioannou, "A comparison of spacing and headway control laws for automatically controlled vehicles," *Vehicle System Dynamics*, vol. 23, no. 1, pp. 597–625, 1994.
- [6] D. Swaroop, "String stability of interconnected systems: An application to platooning in automated highway systems," 1997.
- [7] J. Ploeg, N. Van De Wouw, and H. Nijmeijer, "Lp string stability of cascaded systems: Application to vehicle platooning," *IEEE Transactions on Control Systems Technology*, vol. 22, no. 2, pp. 786–793, 2014.
- [8] J.-W. Kwon and D. Chwa, "Adaptive bidirectional platoon control using a coupled sliding mode control method," *IEEE Transactions on Intelligent Transportation Systems*, vol. 15, no. 5, pp. 2040–2048, 2014.
- [9] Y. Zheng, S. E. Li, J. Wang, D. Cao, and K. Li, "Stability and scalability of homogeneous vehicular platoon: Study on the influence of information flow topologies," *IEEE Transactions on intelligent transportation systems*, vol. 17, no. 1, pp. 14–26, 2015.
- [10] X. Guo, J. Wang, F. Liao, and R. S. H. Teo, "Distributed adaptive integrated-sliding-mode controller synthesis for string stability of vehicle platoons," *IEEE Transactions on Intelligent Transportation Systems*, vol. 17, no. 9, pp. 2419–2429, 2016.
- [11] K. B. Devika, N. Sridhar, V. R. S. Yellapantula, and S. C. Subramanian, "Control of heavy road vehicle platoons incorporating actuation dynamics," in *TENCON 2019-2019 IEEE Region 10 Conference (TENCON)*. IEEE, 2019, pp. 1434–1439.
- [12] D. Yanakiev and I. Kanellakopoulos, "Variable time headway for string stability of automated heavy-duty vehicles," in *Proceedings of 1995 34th IEEE Conference on Decision and Control*, vol. 4. IEEE, 1995, pp. 4077–4081.
- [13] L. Xiao and F. Gao, "Practical string stability of platoon of adaptive cruise control vehicles," *IEEE Transactions on intelligent transportation systems*, vol. 12, no. 4, pp. 1184–1194, 2011.
- [14] Y. Bian, Y. Zheng, W. Ren, S. E. Li, J. Wang, and K. Li, "Reducing time headway for platooning of connected vehicles via v2v communication," *Transportation Research Part C: Emerging Technologies*, vol. 102, pp. 87–105, 2019.
- [15] G. Guo and D. Li, "Adaptive sliding mode control of vehicular platoons with prescribed tracking performance," *IEEE Transactions on Vehicular Technology*, vol. 68, no. 8, pp. 7511–7520, 2019.
- [16] K. B. Devika, G. Rohith, V. R. S. Yellapantula, and S. C. Subramanian, "A dynamics-based adaptive string stable controller for connected heavy road vehicle platoon safety," *IEEE Access*, vol. 8, pp. 209 886–209 903, 2020.
- [17] K. B. Devika, N. Sridhar, H. Patil, and S. C. Subramanian, "Delay compensated pneumatic brake controller for heavy road vehicle active safety systems," *Proceedings of the Institution of Mechanical Engineers, Part C: Journal of Mechanical Engineering Science*, p. 0954406220952822, 2020.
- [18] H. Pacejka, *Tire and vehicle dynamics*. Elsevier, 2005.
- [19] A. A. Hussein and H. A. Rakha, "Vehicle platooning impact on drag coefficients and energy/fuel saving implications," *arXiv preprint arXiv:2001.00560*, 2020.
- [20] K. B. Devika and S. Thomas, "Power rate exponential reaching law for enhanced performance of sliding mode control," *International Journal of Control, Automation and Systems*, vol. 15, no. 6, pp. 2636–2645, 2017.